Sandpiles with height restrictions

Ronald Dickman[1,†], Tânia Tomé[1], and Mário J. de Oliveira[2]

[1] *Departamento de Física, ICEx, Universidade Federal de Minas Gerais, Caixa Postal 702,*
30161-970 Belo Horizonte, MG, Brazil

[2] *Instituto de Física, Universidade de São Paulo, Caixa Postal 66318, 05315-970 São Paulo, SP,*
Brazil

(February 1, 2008)

Abstract

We study stochastic sandpile models with a height restriction in one and two dimensions. A site can topple if it has a height of two, as in Manna's model, but, in contrast to previously studied sandpiles, here the height (or number of particles per site), cannot exceed two. This yields a considerable simplification over the unrestricted case, in which the number of states per site is unbounded. Two toppling rules are considered: in one, the particles are redistributed independently, while the other involves some cooperativity. We study the fixed-energy system (no input or loss of particles) using cluster approximations and extensive simulations, and find that it exhibits a continuous phase transition to an absorbing state at a critical value ζ_c of the particle density. The critical exponents agree with those of the unrestricted Manna sandpile.

Typeset using REVTEX

I. INTRODUCTION

Sandpile models are the prime example of self-organized criticality (SOC) [1,2], a control mechanism that forces a system with an absorbing-state phase transition to its critical point [3–5], leading to scale-invariance in the apparent absence of parameters [6]. SOC in a slowly-driven sandpile corresponds to an absorbing-state phase transition in a model having the same local dynamics, but a fixed number of particles [3,7–10]. The latter class of models have come to be called fixed-energy sandpiles (FES). While most studies of sandpiles have probed the driven case [2,14], there is great interest in understanding the scaling properties of FES models as well [9,11–13]. In this paper we study FES with a height restriction.

From the theoretical standpoint, an inconvenient feature of sandpile models is that the number of particles per site is unbounded. This complicates attempts to derive cluster approximations and continuum descriptions. In Manna's stochastic sandpile [15,16], a site with $z \geq 2$ particles is active, i.e., can topple, sending two particles to neighboring sites. This suggests restricting the number of particles per site to $z = 0$, 1 or 2. In this work we study such a model, in one and two dimensions, with the goal of establishing its critical properties. Analyses of FES without a height restriction reveal that they exhibit a phase transition between an absorbing and an active state as the particle density ζ is increased beyond a critical value [3,17,18]; we find the same to be true of the restricted-height models. Thus the restricted model has nontrivial critical behavior, and represents, due to its simplicity, an attractive system for further theoretical analysis. Moreover, a detailed study allows us to address questions of universality in sandpiles, and, more generally, of absorbing-state phase transitions in systems with a conserved density [19]. The balance of this paper is organized as follows. In Sec. II we define the models, followed by a discussion of cluster approximations in Sec. III. Numerical results are analyzed in Sec. IV, and in Sec. V we summarize our findings.

II. MODELS

The models are defined on a hypercubic lattice with periodic boundaries: a ring of L sites in one dimension, a square lattice of $L \times L$ sites in 2d. The configuration is specified by the number of particles $z_i = 0, 1$, or 2 at each site i; sites with $z_i = 2$ are *active*, and have a toppling rate of unity. The continuous-time (i.e., sequential), Markovian dynamics consists of a series of toppling events at individual sites. (Maintaining the restiction $z \leq 2$ would be quite complicated in a simultaneous-update scheme.) When site i topples, two particles attempt to move to randomly chosen nearest neighbors j and j' of i. (j and j' need not be distinct.) Each particle transfer is accepted so long as it does not lead to a site having more than two particles. The next site to topple is chosen at random from a list of active sites, which must naturally be updated following each event. The time increment associated with each toppling is $\Delta t = 1/N_A$, where N_A is the number of active sites just prior to the event. Δt is the mean waiting time to the next event, if we were to choose sites blindly, instead of using a list. In this way, N_A sites topple per unit time, consistent with each active site having a unit rate of toppling.

We consider two stochastic toppling rules. In one, the two particles released when a site topples move independently. Any particle attempting to move to a site harboring two

2

particles is sent back to the toppling site. (Thus an attempt to send two particles from site j to site k, with $z_k = 1$, results in $z_k = 2$ and $z_j = 1$.) We study this *independent* toppling rule in both one and two dimensions. In the other, *cooperative* rule, transitions that would transfer fewer than the maximum possible number of particles are avoided. The cooperative rule is studied in one dimension only. Transition probabilities for the two rules are listed in Table I.

III. CLUSTER APPROXIMATIONS

We have derived cluster approximations for the independent toppling rule at the one-site (i.e., simple mean-field theory) and two-site levels. While the height restriction complicates the analysis of transitions, it confers the advantage of a strict limit on the the number of variables. (To study the unrestricted sandpile using cluster approximations one must impose a cutoff on the height distribution [3].)

A. One-site approximation

At this level of approximation there are three variables, p_n, with $n = 0, 1$ or 2, representing the probability of a site having exactly n particles. It is convenient to use the shorthand notation $p_n \equiv (n)$. There is only one independent variable, due to the constraints of normalization, $(0) + (1) + (2) = 1$, and of fixed density, $\zeta = (1) + 2(2)$.

We begin the analysis by enumerating, in Fig. 1, the possible transitions between states of a single site. Each transition requires a specific local configuration (of two or three sites, depending on the process), and a particular redistribution of the two particles liberated when the active site topples. The local configuration and the choice of redistribution are independent events. In the one-site approximation all joint probabilities for two or more sites are factorized: $(ij) \rightarrow (i)(j)$ and $(ijk) \rightarrow (i)(j)(k)$.

To illustrate how transition rates are evaluated we consider some examples. The transition $0 \rightarrow 1$ requires the initial configuration $\boxed{0}\ \boxed{2}$, i.e., an empty site with an active neighbor. Exactly one of the two particles must jump to the empty site; in d dimensions this occurs with probability $(2d-1)/2d^2$. Thus the rate of transitions $0{\rightarrow}1$ is

$$2d\frac{2d-1}{2d^2}(0)(2) = \frac{2d-1}{d}(0)(2)$$

where the factor $2d$ represents the number of nearest neighbors.

Consider now the transition $2 \rightarrow 1$. There are two mutually exclusive paths by which it can be realized. In one, both particles jump to the same neighbor (the probability for this event is $1/4d^2$); if the neighbor bears a single particle, then only one particle will be transferred, as required. Thus the initial configuration must be $\boxed{2}\ \boxed{1}$ and the rate for this path is $(2)(1)/2d$. In the other path, the particles jump to distinct sites (the probability for this is $1/2d^2$), one of which must already have two particles, while the other must have fewer than two. The required initial configuration is therefore $\boxed{2}\ \boxed{2}\ \boxed{\not{2}}$, where $\not{2}$ denotes a site with $z < 2$. The rate for this path is $(2-d^{-1})(2)^2(\not{2})$. Evaluating the rates for the remaining transitions we obtain the equations of motion:

3

$$\frac{d}{dt}(0) = \frac{2d-1}{2d}(2)[(2)^2 - 2(0)] \;, \tag{1}$$

$$\frac{d}{dt}(1) = \frac{2d-1}{d}(2)[(0) + (2)(2) - (1)] \tag{2}$$

and

$$\frac{d}{dt}(2) = \frac{2d-1}{2d}(2)[2(1) - (2)^2 - 2(2)(2)] \;. \tag{3}$$

After eliminating the variables (0) and (1), a simple calculation shows that the stationary density of active sites is

$$(2) = 2 - \sqrt{5 - 2\zeta} \tag{4}$$

which implies $\zeta_c = 1/2$ regardless of d.

B. Two-site approximation

The dynamical variables are now the nearest-neighbor (NN) joint probabilities (ij) with $i, j = 0$, 1, or 2. There are four independent variables, due to the symmetry $(ij) = (ji)$ (for $i \neq j$) and the two relations noted previously. The allowed transitions between configurations of a NN pair of sites are shown in Fig. 2.

Consider, for example, the transition $00 \to 01$. The initial configuration must be $\boxed{00}\,\boxed{2}$; its probability, in the two-site approximation, is $(00)(02)/(0)$, where $(02)/(0)$ represents the conditional probability for a NN pair in state 02, given one site in state 0. To realize the transition, exactly one particle must be transferred from the toppling site to its neighbor in the 00 pair; this occurs with probability $(2d-1)/2d^2$, as before. The rate for this process is then given by

$$\frac{(2d-1)^2}{2d^2}\frac{(00)(02)}{(0)}$$

where the additional factor of $2d-1$ represents the number of possible locations for the neighbor in state 2. (Note that in the *loss* term for (00) this rate is multiplied by 2 to account for the mirror-symmetric process.) Proceeding in this manner we obtain the rates for each of the 17 allowed transitions. These are used to generate the equations of motion for the pair probabilities, which are then integrated using a fourth-order Runge-Kutta scheme.

We find $\zeta_c = 0.75$ in 1-d (just as for the unrestricted model), and $\zeta_c = 0.63$ in 2-d. (The corresponding simulation values are 0.92965 and 0.71127, respectively, as discussed in the following section.) The cluster approximation predictions for the active-site density are compared with simulation results in Fig. 3. An interesting qualitative result of the 2-site approximation is that active sites are *anticorrelated*, i.e., $(22) < (2)^2$. This is expected on physical grounds, since, to become active, a site must have a NN that has toppled recently.

4

C. Cooperative rule

For the cooperative rule, the evolution equations for the probabilities (0), (1), and (2) are

$$\frac{d}{dt}(0) = -\frac{1}{2}(020) + (121), \tag{5}$$

$$\frac{d}{dt}(1) = (020) - 2(121), \tag{6}$$

and

$$\frac{d}{dt}(2) = -\frac{1}{2}(020) + (121). \tag{7}$$

To obtain the 1-site approximation we factorize all joint probabilities. There is then only one independent equation, for example,

$$\frac{d}{dt}(2) = -(2)\left[\frac{1}{2}(0)^2 + (1)^2\right]. \tag{8}$$

In the stationary state this gives $(0) = \sqrt{2}(1)$ from which it follows that

$$(2) = \frac{3 + \sqrt{2}}{7}\left[\zeta - (\sqrt{2} - 1)\right]. \tag{9}$$

The critical density is then $\zeta_c = \sqrt{2} - 1 \simeq 0.41421$.

The smaller value of ζ_c here, as compared with the independent rule, reflects the fact the cooperative rule tends to maximize the number of active sites generated. We show below that the critical density ζ_c of the independent model is in fact slightly *lower* than that of the cooperative one. The reason for this is not immediately apparent from the transition rates, but would appear to lie in subtle correlations induced by the dynamics, that are not evident at the 1-site level.

IV. SIMULATION RESULTS

A. Independent rule

We performed extensive simulations of the height-restricted FES with independent toppling rule in one and two dimensions. The initial condition is generated by distributing ζL^d particles randomly among the L^d sites, avoiding occupancy of any site by more than two particles. This yields an initial distribution that is spatially homogeneous, and uncorrelated. The dynamics begins once all the particles have been placed on the lattice. The particle number is, of course, conserved by the dynamics.

In one dimension we study system sizes ranging from $L = 100$ to 5000 sites; in two dimensions the system comprises $L \times L$ sites with $L = 10, 20, 40,...,320$. For each L we study a range of particle densities $\zeta \equiv N/L^d$. The simulations consist of N_s independent

5

runs, extending to a maximum time t_m. (In one dimension, for example, we used $N_s = 10^5$, $t_m = 4000$ for $L = 100$, and $N_s = 2000$, $t_m = 2 \times 10^6$, for $L = 5000$. In two dimensions these parameters varied from $N_s = 10^5$, $t_m = 1000$, for $L = 10$, to $N_s = 2 \times 10^4$ and $t_m = 8 \times 10^4$ for $L = 320$.)

Our first task is to locate the critical density ζ_c; to this end we study the active-site density $\rho_a(t)$, its second moment $\overline{\rho_a^2}(t)$, and the survival probability $P(t)$. The second moment is used to evaluate the ratio $m(t) \equiv \overline{\rho_a^2}(t)/\rho_a^2(t)$. Figures 4 and 5 show typical results for $\rho_a(t)$ and $P(t)$, respectively. $\rho_a(t)$ relaxes to a well-defined stationary value, $\rho_a(\zeta, L)$, (similarly for m), while the exponential decay of of $P(t)$ allows one to extract an associated lifetime, $\tau(\zeta, L)$. The stationary values, $\rho_a(\zeta, L)$ and $m(\zeta, L)$ are obtained by discarding the initial, transient portion of the data, and performing averages over the remainder, weighted by $P(t)$, which measures the effective sample size.

In a fixed-energy sandpile of linear extent L, we can only vary ζ in increments of $1/L^d$. To circumvent this limitation, work we adopt a strategy employed in a recent study of the pair contact process [20]. Given simulation results for the stationary values of ρ_a and m, and of the survival time τ, for a certain system size, we form least-squares cubic fits to these data, permitting interpolation to arbitrary ζ values within the interval studied. Thus, for each L, we regard ρ_a, m, and τ as a functions of a *continuous* variable ζ. (Since the properties of a finite system are nonsingular, the interpolation procedure seems quite natural.) Data sets for m, and associated cubic fits, are shown in Fig. 6.

A well known criterion for criticality is size-independence of order-parameter moment ratios, typically in the form of "crossings" of Binder's reduced fourth cumulant [21]. Moment-ratio crossings have also proven useful for fixing the critical parameter value at absorbing-state phase transitions [20,22,23]. We determine the value $\zeta_{cr}(L, L')$ for which $m(\zeta, L) = m(\zeta, L')$, for successive L values. Extrapolating these data to $L \to \infty$ yields our estimate for ζ_c; Fig. 7 illustrates the procedure. Evidently the crossing values $\zeta_{cr}(L, L')$ converge quite rapidly. In two dimensions, the crossings are well described by the form $\zeta_{cr}(L, L') \simeq \zeta_c + aL^{-b}$ where a is an amplitude and $b \simeq 2.72$.

Analysis of the moment-ratio crossings yields $\zeta_c = 0.92965(3)$ in 1-d and $\zeta_c = 0.711270(3)$ in 2-d, where the figures in parentheses denote uncertainties. For comparison, we note the values for the *unrestricted* version of the model: $0.94885(7)$ in 1-d, $0.71695(5)$ in 2-d. Thus the height restriction yields a rather small shift in ζ_c, by about 2% in one dimension, and 0.8% in 2-d. This is reasonable since, in the unrestricted model (near its critical point), only a small fraction of the sites have $z > 2$. The critical values of the moment ratio are: $m_c = 1.1596(4)$ in 1-d, and $1.347(2)$ in 2-d. While these differ significantly from the corresponding values for the directed percolation (DP) universailty class [$1.1735(5)$ and $1.3257(5)$ in 1-d and 2-d, respectively [22]], the moment ratios for the two classes are very similar.

In studies of absorbing-state phase transitions [24], including fixed-energy sandpiles [9,18], it is common to determine the critical point by seeking a power-law dependence of the order parameter (ρ_a in the present instance) and the relaxation time on the system size L. The former is governed by

$$\rho_a(\zeta, L) = L^{-\beta/\nu_\perp} \mathcal{R}(L^{1/\nu_\perp} \Delta) , \tag{10}$$

as expected on the basis of finite-size scaling [25]. (Here $\Delta \equiv \zeta - \zeta_c$, and $\mathcal{R}$ is a scaling

function.) Thus at the critical point ($\Delta = 0$) we expect $\rho_a(\zeta_c, L) \sim L^{-\beta/\nu_\perp}$; for the lifetime one has $\tau(\zeta_c, L) \sim L^{\nu_\parallel/\nu_\perp}$.

With ζ_c in hand, we may verify the power-law dependence of the order parameter and the lifetime on system size, as in Eq. (10), by interpolating the simulation data to the critical value ζ_c. Figure 8 shows that ρ_a indeed has a power-law dependence on L; a similar plot (not shown) yields the same conclusion for τ. From the data for the four largest systems, we then obtain (via least-squares linear fits), the exponent ratios $\beta/\nu_\perp$ and $\nu_\parallel/\nu_\perp$ listed in Table II. (The uncertainties reflect two contributions: one due to the uncertainty of the fit, the other, dominant one, due to the uncertainties in the values of ρ_a and τ for each L. The latter includes the effects of uncertainty in ζ_c.)

To determine the exponent β we analyze the results for ρ_a in the portion of the supercritical regime where the graph of $\ln \rho$ versus $\ln \Delta$ follows a power law. In two dimensions this procedure yields $\beta = 0.661(3)$, $0.661(2)$, $0.654(3)$, and $0.655(2)$ for $L = 20$, 40, 80, and 160, respectively, leading to an estimate of $\beta = 0.656(5)$. Fig. 9, a scaling plot of $L^{\beta/\nu_\perp} \rho_a(\zeta, L)$ versus $L^{1/\nu_\perp} \Delta$ for various system sizes, shows a good data collapse, verifying the finite-size scaling hypothesis for the order parameter, and yielding $\nu_\perp = 0.85$.

In one dimension it turns out that no power laws are seen if we use $\zeta_c = 0.92965$ as determined from the FSS analysis described above. Quite clean power law dependence of ρ_a is observed, however, if we use an L-dependent *effective* critical point $\zeta_{c,L}$ in the analysis. We determine $\zeta_{c,L}$ by optimizing the linearity of $\ln \rho_a$ as a function of $\ln \Delta$, and maximizing the number of data points that may reasonably be fit by the power law. (For $L = 1000$ for example, we are able to fit 15 points with a correlation coefficient of 0.99996.) The resulting values of $\zeta_{c,L}$ and β are listed in Table III. Extrapolating the effective critical densities to infinite L (via linear regression versus $L^{-1/\nu_\perp}$) yields $\zeta_c = 0.9298(4)$, consistent with our our estimate based on moment-ratio crossings. A similar extrapolation gives $\beta = 0.412(4)$ We determine the exponent $\nu_\perp$ via a data-collapse analysis, as in the 2d case (see Fig. 10). We obtain a good data collapse for $1/\nu_\perp$ in the range 0.60 to 0.62, leading to the estimate $\nu_\perp = 1.64(4)$.

B. Cooperative rule

We performed extensive simulations of the cooperative model in one dimension with system sizes again ranging from $L = 100$ to $L = 5000$. In this case we prevented the system from falling into an absorbing configuration by maintaing at least two active sites. (If there are only two active sites, transitions which decreases the number of active sites are not permitted. Actually, there is only one transition of this sort, $020 \to 101$.) The density of active sites ρ is then always $\geq 2/L$. But since the stationary value of ρ_a at the critical point is $\sim L^{-\beta/\nu_\perp}$, with $\beta/\nu_\perp \simeq 1/4$, this should have a minimal effect on critical properties. Figure 11 shows the stationary active-site density as a function of the particle density for several values of L.

We first analyzed the stationary critical properties of the model by means of the finite size scaling relation, Eq. (10). The critical density was obtained by plotting ρ_a versus L for several ζ values, as shown in Fig. 12. (As before, values of ρ_a for densities between those accessible for a given L were obtained via interpolation.) Using the criterion of power law dependence of the order parameter on system size, we find $\zeta_c = 0.9788(1)$ and $\beta/\nu_\perp =$

0.245(5). As an alternative determination of ζ_c we used moment-ratio crossings. Figure 13 shows the moment ratio m as a function of ζ for $L = 2000$ and $L = 5000$. The two curves cross at $\zeta_c = 0.9788$, confirming the previous result.

Having obtained the critical particle density, we used it to find the critical exponent β governing the order parameter. Figure 14 is a log-log plot of ρ_a versus $\zeta - \zeta_c$ for several values of L. The slope of the straight line fitted to the data points for $L = 5000$ gives $\beta = 0.417(1)$. From this, and our previous result for $\beta/\nu_\perp$, we obtain $\nu_\perp = 1.70(4)$.

We also performed time-dependent simulations at the critical density, to measure the growth of the number of active sites. Here, each trial began with just one active site. For a given particle density ζ, this was realized by placing a particle at each of $\zeta L - 1$ distinct sites, chosen at random. One of these sites was then selected randomly, and another particle placed there, rendering it active. In a lattice of size $L = 10000$, we performed from 5000 to 6000 trials of this kind, to determine the mean number of particles, $n(t)$, averaged over all trials (including those that fall into an absorbing configuration prior to time t). At the critical point, and for a sufficient large system, $n(t)$ is expected to increase asymptotically as a power law

$$n(t) \sim t^\eta \tag{11}$$

where the exponent η is related to the exponent $z = \nu_\parallel/\nu_\perp$ by the scaling relation [11,26],

$$z = \frac{1}{\eta}\left(d - 2\frac{\beta}{\nu_\perp}\right), \tag{12}$$

in d dimensions. Our data for $n(t)$ at $\zeta_c = 0.9788$ do in fact follow a power law, and yield the estimate $\eta = 0.330(5)$. Using our previous result for $\beta/\nu_\perp$ we then obtain $z = 1.54(5)$.

V. DISCUSSION

We studied the scaling behavior of fixed-energy sandpiles that follow a stochastic dynamics similar to that of the Manna model, but with a height restriction $z_i \le 2$. Both versions of the model (i.e., the independent and cooperative toppling rules), exhibit a continuous phase transition between an absorbing state and an active one at a critical particle density ζ_c. One- and two-site cluster approximations do not yield very accurate predictions for the critical density (as is to be expected), but they correctly predict the continuous nature of the transition.

As shown in Table II, the critical exponents for the present models appear to be the same as for the unrestricted case. In fact, there is excellent agreement between the exponent values for the restricted and unrestricted models, except for the exponent $z = \nu_\parallel/\nu_\perp$ in one dimension. As was noted in Ref. [18], however, obtaining a reliable estimate for the exponent z from simulations is quite difficult in one dimension. (In two dimensions the estimates for z are in excellent agreement. It appears that the relaxation dynamics is anomalous in one dimension, as suggested in [18].)

Studies of a reaction model suggest a common universality class, distinct from that of directed percolation, for absorbing-state phase transitions in which the order parameter is coupled to a second field that relaxes diffusively in the presence of activity [19]. Manna's

stochastic sandpile falls in this category, with the local particle density $\zeta(\mathbf{x}, t)$ playing the role of the second field. Our results show that height restrictions and perturbations of the toppling rule do not alter the critical exponents, if they preserve the above-mentioned features, supporting universality in critical behavior far from equilibrium.

Acknowledgements

†email: dickman@fisica.ufmg.br

REFERENCES

[1] P. Bak, C. Tang and K. Wiesenfeld, Phys. Rev. Lett. **59**, 381 (1987); Phys. Rev. A **38**, 364 (1988).

[2] D. Dhar, Physica A **263** (1999) 4, and references therein.

[3] R. Dickman, M. A. Muñoz, A. Vespignani, and S. Zapperi, Braz. J. Phys. **30**, 27 (2000). e-print: cond-mat/9910454.

[4] M. A. Muñoz, R. Dickman, R. Pastor-Satorras, A. Vespignani, and S. Zapperi, in *Modeling Complex Systems*, Proceedings of the 6th Granada Seminar on Computational J. Marro and P. L. Garrido, eds., AIP Conference Proceedings v. 574 (2001); e-print: cond-mat/0011442.

[5] R. Dickman, Physica A, in press; e-print: cond-mat/0110043.

[6] G. Grinstein, in *Scale Invariance, Interfaces and Nonequilibrium Dynamics, NATO Advanced Study Institute, Series B: Physics*, vol. 344, A. McKane et al., Eds. (Plenum, New York, 1995).

[7] C. Tang and P. Bak, Phys. Rev. Lett. **60**, 2347 (1988).

[8] A. Vespignani and S. Zapperi, Phys. Rev. Lett. **78**, 4793 (1997); Phys. Rev. E **57**, 6345 (1998).

[9] R. Dickman, A. Vespignani and S. Zapperi, Phys. Rev. E **57**, 5095 (1998).

[10] A. Vespignani, R. Dickman, M. A. Muñoz, and Stefano Zapperi, Phys. Rev. Lett. **81**, 5676 (1998).

[11] M. A. Muñoz, R. Dickman, A. Vespignani, and Stefano Zapperi, Phys. Rev. E **59**, 6175 (1999).

[12] A. Chessa, E. Marinari and A. Vespignani, Phys. Rev. Lett. **80**, 4217 (1998).

[13] A. Montakhab and J. M. Carlson, Phys. Rev. E **58**, 5608 (1998).

[14] V. B. Priezzhev, J. Stat. Phys. **74**, 955 (1994); E. V. Ivashkevich, J. Phys. A **27**, 3643 (1994); E. V. Ivashkevich,D.V.Ktitarev and V. B. Priezzhev, Physica A **209**, 347 (1994).

[15] S. S. Manna, J. Phys. A **24**, L363 (1991).

[16] S. S. Manna, J. Stat. Phys. **59**, 509 (1990).

[17] A. Vespignani, R. Dickman, M. A. Muñoz, and S. Zapperi, Phys Rev. E**62**, 4564 (2000).

[18] R. Dickman, M. Alava, M. A. Muñoz, J. Peltola, A. Vespignani, and S. Zapperi, Phys Rev. E**64**, 056104 (2001).

[19] M. Rossi, R. Pastor-Satorras, and A. Vespignani, Phys. Rev. Lett. 85 (2000) 1803.

[20] R. Dickman, W. M. Rabêlo, and G. Ódor, Phys. Rev. E **65**, 016118 (2002).

[21] K. Binder, Phys. Rev. Lett. **47**, 693 (1981); Z. Phys. B**43**, 119 (1981).

[22] R. Dickman and J. Kamphorst Leal da Silva, Phys Rev. E**58**, 4266 (1998).

[23] J. Kamphorst Leal da Silva and R. Dickman, Phys Rev. E **60**, 5126 (1999).

[24] J. Marro and R. Dickman *Nonequilibrium Phase Transitions in Lattice Models* (Cambridge University Press, Cambridge, 1999).

[25] M. E. Fisher, in *Proceedings of the International Summer School 'Enrico Fermi', Course LI*, (Academic Press, New York, 1971); M. E. Fisher and M. N. Barber, Phys. Rev. Lett. **28**, 1516 (1972).

[26] P. Grassberger and A. de la Torre, Ann. Phys. (N.Y.) **122**, 373 (1979).

Transition	Probability	
	Independent	Cooperative
$020 \rightarrow 101$	1/2	1/2
$\rightarrow 200$	1/4	1/4
$\rightarrow 002$	1/4	1/4
$120 \rightarrow 201$	1/2	1/2
$\rightarrow 102$	1/4	1/2
$\rightarrow 210$	1/4	0
$220 \rightarrow 202$	1/4	1
$\rightarrow 211$	1/2	0
$\rightarrow 220$	1/4	0
$121 \rightarrow 202$	1/2	1
$\rightarrow 112$	1/4	0
$\rightarrow 211$	1/4	0
$122 \rightarrow 212$	3/4	1
$\rightarrow 122$	1/4	0

Table I. Transition probabilities for the independent and cooperative toppling rules in one dimension. The transition probabilities are symmetric under reflection.

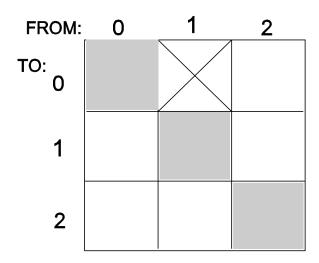| Model	ζ_c	$\beta/\nu_\perp$	$\nu_\parallel/\nu_\perp$	β
Indep. 1d	0.92965(3)	0.247(2)	1.45(3)	0.412(4)
Coop. 1d	0.9788(1)	0.245(5)	1.54(5)	0.417(1)
Unrst. 1d	0.94885(7)	0.239(11)	1.66(7)	0.42(2)
Indep. 2d	0.711270(3)	0.774(3)	1.572(7)	0.656(5)
Unrst. 2d	0.71695(5)	0.78(2)	1.57(4)	0.64(1)

Table II. Critical parameters of restricted and unrestricted sandpiles. Figures in parentheses denote uncertainties. Results for the unrestricted models are from Refs. [18] (1-d) and [17] (2-d).

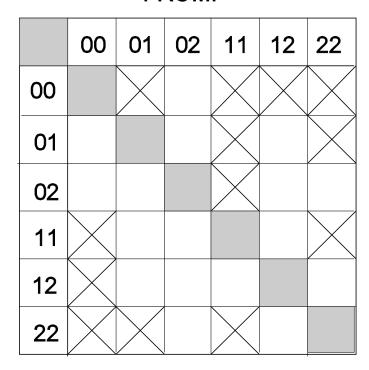| L	$\zeta_{c,L}$	β_L
500	0.9256(1)	0.465(3)
1000	0.9273(1)	0.441(4)
2000	0.92815(5)	0.431(4)
2000	0.92845(5)	0.423(4)
∞	0.9298(4)	0.412(4)

Table III. Effective size-dependent critical density and apparent exponent β_L, and $L \rightarrow \infty$ extrapolated values, for the 1-d model with independent toppling rule.

FIGURE CAPTIONS

FIG. 1. Transitions between states of a single site. '$\times$' denotes a forbidden transition; diagonal entries are irrelevant.

FIG. 2. Transitions between configurations of a NN pair of sites; '$\times$' denotes a forbidden transition; diagonal entries are irrelevant.

FIG. 3. The stationary active-site density in the two-dimensional restricted-height sandpile as predicted by the one-site and two-site approximations, compared with the simulation result.

FIG. 4. Evolution of the active-site density in the one-dimensional sandpile with height restriction (independent rule). $L=1000$; $\zeta=0.93$.

FIG. 5. Evolution of the survival probability $P(t)$, for the same parameters as in Fig. 4.

FIG. 6. Stationary moment ratio, $m(\zeta)$, in the one-dimensional model (independent rule). Squares: $L=500$; $+$: $L=2000$. Curves are cubic fits to the data.

FIG. 7. Moment-ratio crossing values ζ_{cr} versus reciprocal system size in 1-d (independent rule).

FIG. 8. Stationary active-site density ρ_a versus system size L at the critical point in 1-d ($+$) and 2-d (squares) (independent rule).

FIG. 9. Scaling plot of the stationary active-site density in the 2-d (independent rule). System sizes $L=20$ (filled squares), 40 (open squares), 80 ($\times$) and 160 ($+$).

FIG. 10. Scaling plot of the stationary active-site density in 1-d (independent rule). System sizes $L=500$ ($\circ$), 1000 ($\diamond$), 2000 ($\times$) and 5000 ($+$).

FIG. 11. Stationary active-site density in 1-d versus particle density, for various system sizes (cooperative rule).

FIG. 12. Stationary active-site density versus system size in 1-d (cooperative rule).

FIG. 13. Stationary moment ratio in the one-dimensional model (cooperative rule).

FIG. 14. Stationary active-site density versus $\zeta-\zeta_c$ for various system sizes (cooperative rule, 1-d).

FROM:

TO:	00	01	02	11	12	22
00	▨	X		X	X	X
01		▨		X		X
02			▨	X		
11	X			▨		X
12	X				▨	
22	X	X		X		▨